Precise determination of the $X(3872)$ properties

Xiang-Kun Dong
In collaboration with T. Ji, F.-K. Guo, C. Hanhart and U.-G. Meißner

HISKP, Bonn University

Oct. 24, 2024

Implications of LHCb measurements and future prospects
Oct. 23-25, 2024, CERN

Contents

The Thriving Hadron Spectrum: Challenges! Chances!!!

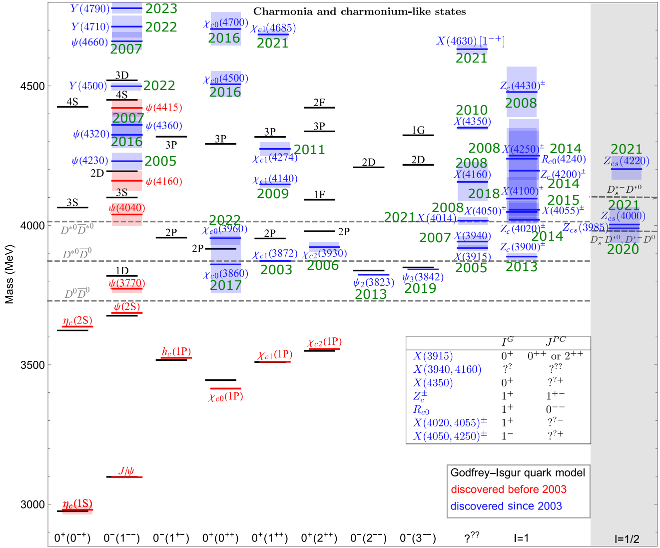

Figure: Spectrum of charmonium(-like) states up to 2023.
Plot courtesy of Feng-Kun Guo.

What are they?

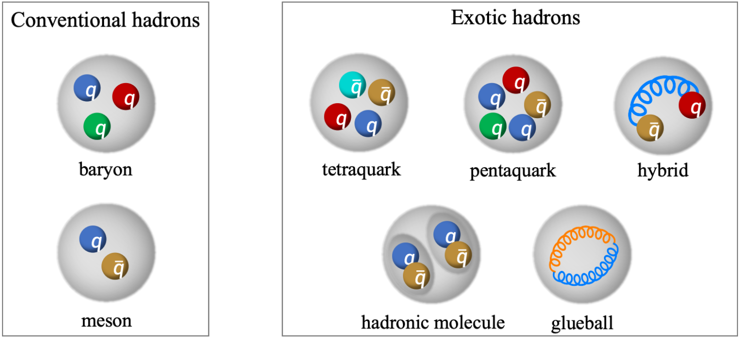

Figure: Illustration of hadron structures. Plot courtesy of Feng-Kun Guo.

Low-energy QCD, non-perturbative.

Recent reviews: A. Esposito, et al. arXiv:1611.07920; F.-K. Guo, et al. arXiv:1705.00141; S. L. Olsen, et al. arXiv:1708.04012; Y.-R. Liu, et al. arXiv:1903.11976; N. Brambilla, et al. arXiv:1907.07583; Hua-Xing Chen, et al. arXiv:2204.02649. (Many others not listed here. Sorry!)

Congratulations to the Great Achievements at the LHC

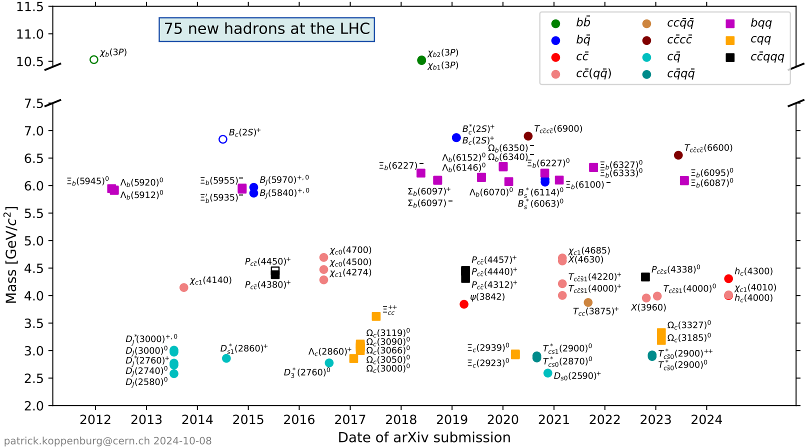

Figure: 75 new hadrons at the LHC up to 2024-10-08.

https://www.nikhef.nl/~pkoppenb/hadrons/Masses.pdf

Plot courtesy of Patrick S. Koppenburg.

What a Charming Scenery!

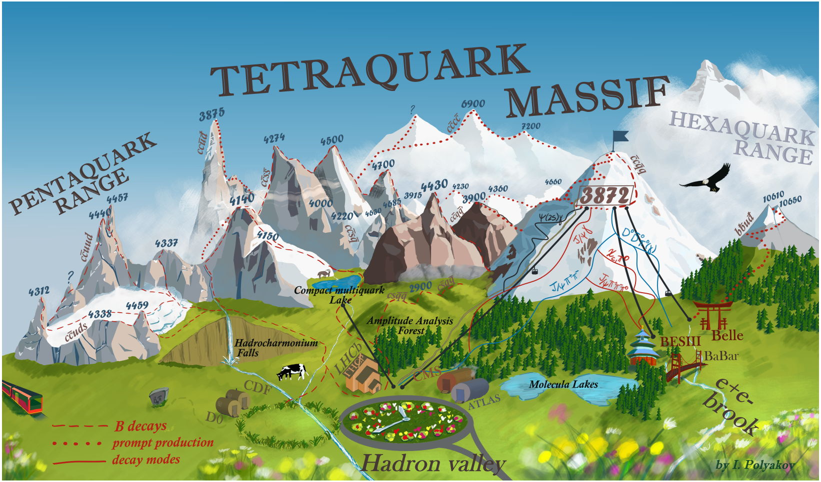

Figure: Illustration of exotic hadron experimental studies.

N. Hüsken, E. S. Norella and I. Polyakov, arXiv:2410.06923.

Figure courtesy of Ivan Polyakov.

Let's go to the superstar $X(3872)$

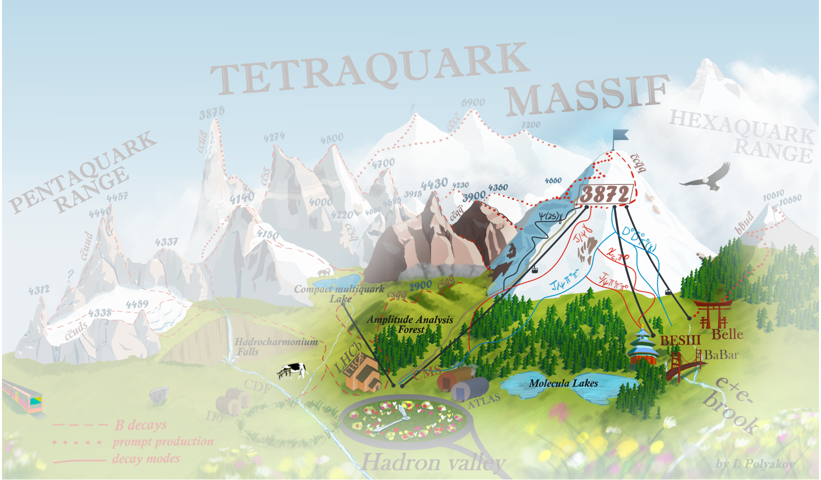

Figure: Illustration of exotic hadron experimental studies.

N. Hüsken, E. S. Norella and I. Polyakov, arXiv:2410.06923.

Figure courtesy of Ivan Polyakov.

Contents

Profile of the Superstar $X(3872)$

- "Born" in 2003 at Belle. Followed by many other experiments.
  ~~One of~~ the most famous member in exotic hadron community. Most studied.
- Observed channels: $J/\psi\rho/\omega(2\pi/3\pi)$, $J/\psi\gamma$, $\psi(2S)\gamma$, $\chi_{cJ}(1P)\pi^0$, $D^0\bar{D}^{*0}(\to D^0\bar{D}^0\pi^0/\gamma)$.
- Mass and width very different from $c\bar{c}$.
  - Mass, 3871.64 ± 0.06 MeV(PDG), exactly at $D^0\bar{D}^{*0}$ threshold.
  - Tiny decay width, 1.19 ± 0.21 MeV(PDG).
  - Breit-Wigner, well-known IMPROPER!
  - Flatté, LHCb, arXiv:2005.13419, BESIII, arXiv:2309.01502,

$$E_X \sim \begin{cases} (25 - 140i) \text{ keV (LHCb)} \\ (0 - 190i) \text{ keV (BESIII)} \end{cases} .$$

Improved but NOT enough!

  - Call for more reliable parameterization.

Unitarity and analyticity; Coupled channels; $D\bar{D}\pi$ 3-body effects; Production information.

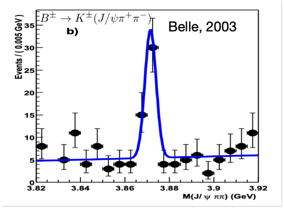

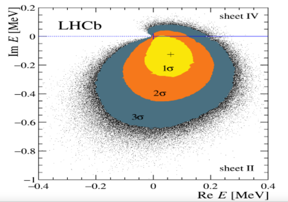

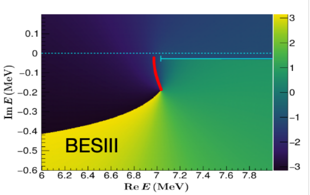

(a) sheet I: $E_{\text{I}} = 7.04 - 0.19i$ MeV

Parameterization of near-threshold lineshapes
Two channels, LO NREFT X.-K. Dong, et al. arXiv:2011.14517

- At leading order

$$T(E) = 8\pi\Sigma_2 \begin{pmatrix} -\frac{1}{a_{11}} + ik_1 & \frac{1}{a_{12}} \\ \frac{1}{a_{12}} & -\frac{1}{a_{22}} - \sqrt{-2\mu_2 E - i\epsilon} \end{pmatrix}^{-1}$$

$$= -\frac{8\pi\Sigma_2}{\det} \begin{pmatrix} \frac{1}{a_{22}} + \sqrt{-2\mu_2 E - i\epsilon} & \frac{1}{a_{12}} \\ \frac{1}{a_{12}} & \frac{1}{a_{11}} - ik_1 \end{pmatrix},$$

with $\det = (1/a_{11} - i\,k_1)\left(1/a_{22} + \sqrt{-2\mu_2 E - i\epsilon}\right) - 1/a_{12}^2$.

- Production amplitude of channel-1, the observing channel,

$$P_1^\Lambda[1 + G_1^\Lambda T_{11}(E)] + P_2^\Lambda G_2^\Lambda(E) T_{21}(E) = P_1 T_{11}(E) + P_2 T_{21}(E).$$

Energy dependence only in T_{11} and T_{21}.

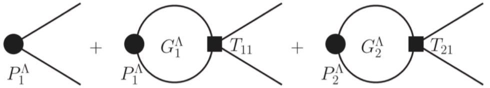

- For symmetry-related two-channel system, see Z.-H. Zhang, et al. arXiv:2407.10620.

Near-(2nd)threshold lineshapes

Highly depends on production ratio. X.-K. Dong, et al. arXiv:2011.14517

(a) T_{21} driven, $P_2 \gg P_1$

- Virtual state: peak at threshold;
- Bound state: peak below threshold;
- Attraction: near-threshold peak.

(b) T_{11} driven, $P_1 \gg P_2$

- Universal dip for strong S-wave attraction in channel-2;
- $T_{11} \propto \frac{1}{a_{22}} + \sqrt{-2\mu_2 E - i\epsilon}$.

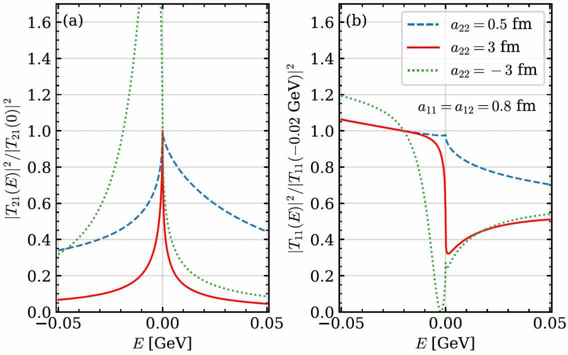

OPE enters, solving LSE (integral form) directly.

Profile of the Superstar $X(3872)$

- $J^{PC} = 1^{++}$ LHCb, arXiv:1302.6269. But properties not match $\chi_{c1}(2P)$.
- Isospin-0, no charged partner observed. $I = 1$ W_{c1}, mild cusp as virtual states. χEFT Z. H. Zhang, et al. arXiv:2404.11215, LQCD M. Sadl, et al. arXiv:2406.09842. Data lacks sufficient statistics.
- Large isospin breaking in the decay, $\mathrm{Br}(J/\psi 3\pi)/\mathrm{Br}(J/\psi 2\pi)$

$$\begin{cases} 1.0 \pm 0.4 \pm 0.3 & \text{Belle}, \\ 0.7 \pm 0.3\,(1.7 \pm 1.3) & \text{BaBar } B^+\,(B^0), \\ 1.6^{+0.4}_{-0.3} \pm 0.2 & \text{BESIII}\,, \end{cases}$$

- PhSp difference. More natural measurement of isospin breaking, $R_X \equiv g_{X\psi\rho}/g_{X\psi\omega}$ M. Suzuki, arXiv:hep- ph/0508258. How large is it?
- Her nature: more likely a $D^0\bar{D}^{*0}$-D^+D^{*-} molecule but still in debate. Compositeness. Productions. Decays.

BaBar, arXiv: hep-ex/0412051

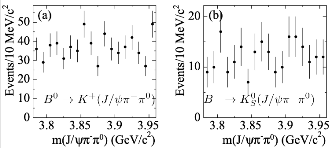

Belle, arXiv:1107.0163

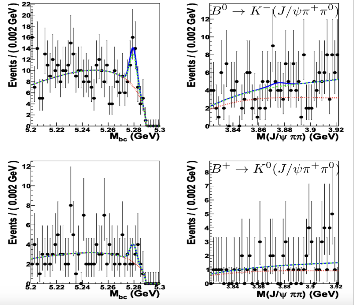

Isospin breaking in the $X(3872)$ decays

- $\mathrm{Br}(J/\psi 3\pi)/\mathrm{Br}(J/\psi 2\pi)$, mediated by ρ and ω, BW,
  $R_X = 0.29 \pm 0.02$ M. Suzuki, arXiv:hep-ph/0508258
  $R_X = 0.30 \pm 0.07$ E. Braaten, et al. arXiv:hep-ph/0507163.
- Distribution of 3π and 2π, ρ-ω mixing,
  $R_X = 0.26^{+0.08}_{-0.05}$ C. Hanhart, et al. arXiv:1111.6241.
- Much more precious 2π distribution, coupled 2π-3π, ρ and ω BW,
  $R_X = 0.29 \pm 0.04$ LHCb, arXiv:2204.12597.
- ρ and ω BW + dipole FF, for running or constant ρ width,
  $R_X = (0.25 \text{ or } 0.30) \pm 0.01$ H.-N. Wang, et al. arXiv:2206.14456.
- Best available ρ spectral function,
  Omnès instead of BW, (Diff. by ∼0.03)

$$\mathcal{M}_{2\pi} = q_\pi\, P(s)\, \Omega(s) \left[1 - \frac{\epsilon_{\rho\omega}}{R_X}\, G_\omega(s)\right],$$

$$\varepsilon_{\rho\omega} = 3.4 \times 10^{-3}\ \mathrm{GeV}^2.$$

$R_X = 0.28 \pm 0.03$ J. M. Dias, et al. arXiv:2409.13425.

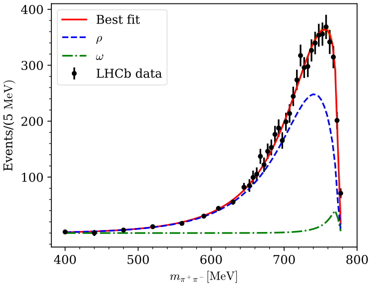

- Possible W^0_{c1} contribution?

Internal structure of the $X(3872)$

- Far beyond quark model predictions for $\chi_{c1}(2P)$.

Compact tetraquark $[c\bar{c}q\bar{q}]$

- Fine tuning.
- Three partners. No evidence.
- Large isospin breaking.
- Strong coupling to $D^0\bar{D}^{*0}$.

$D^0\bar{D}^{*0}$ molecule

- Fine tuning, but not that much.
- Prompt production. Short range.
- $\frac{\mathrm{Br}(X(3872)\to\psi'\gamma)}{\mathrm{Br}(X(3872)\to J/\psi\gamma)}$. Short range.
- Large negative r_0. Positive here.

- Compositeness $X(\bar{X}_A) = 1 - Z$, S. Weinberg, Phys.Rev.137,B672(1965).

$$a_0 = -2\left(\frac{1-Z}{2-Z}\right)\frac{1}{\gamma} + \mathcal{O}\left(\frac{1}{\beta}\right), r_0 = -\left(\frac{Z}{1-Z}\right)\frac{1}{\gamma} + \mathcal{O}\left(\frac{1}{\beta}\right),$$

  - $Z = 0, 1$ for pure molecule or compact,

$$a \to -\frac{1}{\gamma} \& r \to \frac{N_r}{\beta}\ (Z\to 1), \quad a \to -\frac{N_a}{\beta} \& r \to -\infty\ (Z \to 0).$$

  - Large negative r_0 $\Rightarrow$ compact component in $X(3872)$?
    LHCb, BESIII and Belle data. LHCb, arXiv:2204.12597; BESIII, arXiv:2309.01502; A. Esposito, et al. arXiv:2108.11413; H. Xu, et al.arXiv:2401.00411.
    Flatté, large uncertainty.
  - To extract X precisely using more reliable parameterization.

Contents

Dynamics of the $X(3872)$

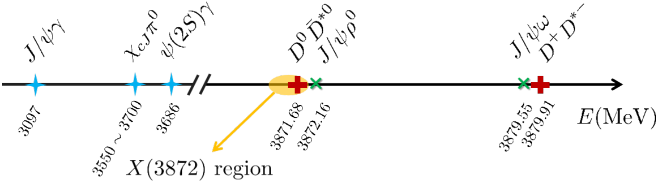

- Hadron-hadron interactions: Pole of scattering amplitudes.
- Elastic channels, strongly coupled to $X(3872)$. Tiny PhSp, large BR.
  $D^0\bar{D}^{*0}$, D^+D^{*-}. ($D\bar{D}\pi/\gamma$).
- Inelastic channels, weakly coupled to $X(3872)$. EM or OZI suppressed.
  - $J/\psi\rho$ and $J/\psi\omega$. Close to $X(3872)$. $J/\psi 2\pi$ and $J/\psi 3\pi$;
  - $J/\psi\gamma$, $\psi(2S)\gamma$, $\chi_{cJ}(1P)\pi^0$: far beyond the $X(3872)$ energy region.
- Chiral effective field theory, near $D\bar{D}^*$ thresholds,
  Contact + OPE.

Lippmann-Schwinger equation

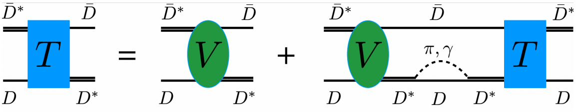

- $D^0\bar{D}^{*0}$-D^+D^{*-} scattering amplitude,

$$T_{\alpha\beta}(E;p',p) = V_{\alpha\beta}(E;p',p) + \int_0^\Lambda \frac{l^2\,dl}{2\pi^2} V_{\alpha\mu}(E;p',l)\,G_{\mu\nu}(E;l)\,T_{\nu\beta}(E;l,p).$$

- Two-body loop propagators, D^* self-energy considered,

$$G_{\alpha\beta}(E;l) = \frac{\delta_{\alpha\beta}}{E - \Delta_{\alpha 1} - \frac{l^2}{2\mu_\alpha} + \frac{i}{2}[\Gamma_\alpha(E;l) + \Gamma_\alpha^{\rm rad}]}.$$

$\Gamma_\alpha(E;l)$, $\Gamma_\alpha^{\rm rad}$, the strong and radiative widths of channel-α.

- Hard cutoff $\Lambda = 1$ GeV. Small cutoff-dependence of physical quantities, numerically checked for $\Lambda = 0.6 \sim 1.4$ GeV.
- Three contributions to the potential,

$$V(E;p',p) = V^{\rm ct} + V^\pi(E;p',p) + V^{\rm inel}(E)\,.$$

Potentials

- Contact interaction, HQSS, 2 LECs, C. Hidalgo-Duque, et al., arXiv:1210.5431.

$$V^{\rm ct} = \frac{1}{2}\begin{pmatrix} C_{0X}+C_{1X} & C_{0X}-C_{1X} \\ C_{0X}-C_{1X} & C_{0X}+C_{1X} \end{pmatrix}.$$

- OPE, onshell, TOPT
  Chiral Lag. for $D^*D\pi$ coupling, $\Gamma_{D^*\to D\pi}$.

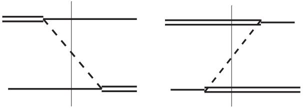

- Effective potential from inelastic loops, C. Hanhart, et al., arXiv:1507.00382

$$V^{\rm inel}_{\alpha\beta}(E) = v_{\alpha j}(s)\,G_{jk}(E)\,v_{k\beta}(s) \\ \to -i\,v_{\alpha j}(s)\rho_{jk}(E,s)\,v_{k\beta}(s).$$

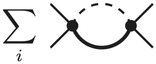

  - Real part absorbed by $V^{\rm ct}$.
  - Elastic-inelastic transitions, $v_{\alpha j}(s) = (1+as)\,u_{\alpha k}\begin{pmatrix} 1 & \epsilon_{\rho\omega}\,G_\rho(s) \\ \epsilon_{\rho\omega}\,G_\omega(s) & 1 \end{pmatrix}_{kj}$
  - ρ-ω mixing considered C. Hanhart, et al. arXiv:1111.6241.
  - Dispersive treatment of ρ, Omnès instead of BW J. M. Dias, et al. arXiv:2409.13425.
  - Other channels, PhSp flat, constant contributions. Neglected.

Production amplitudes

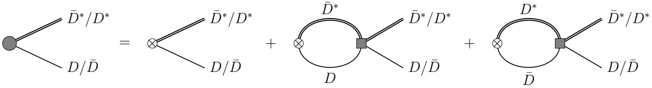

- Production of elastic channels

$$U_\alpha(E,p) = P_\alpha + \int_0^\Lambda \frac{l^2 \mathrm{d}l}{2\pi^2} P_\mu G_{\mu\nu}(E,l) T_{\nu\alpha}(E;l,p).$$

- Production of $D^0 \bar{D}^0 \pi^0$

$$T_{D^0 \bar{D}^0 \pi^0}(E,p,\bar{p}) = U_\alpha(E,p) F_\alpha(p) + U_\alpha(E,\bar{p}) F_\alpha(\bar{p}),$$

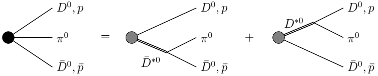

- Production of $J/\psi\pi\pi$

$$T_{J/\psi\pi\pi}(E,s) = \int_0^\Lambda \frac{l^2 \mathrm{d}l}{2\pi^2} U_\alpha(E,l) G_{\alpha\beta}(E,l) H_\beta(s),$$

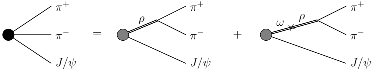

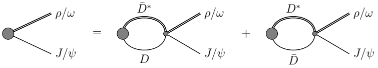

Fitted lineshapes

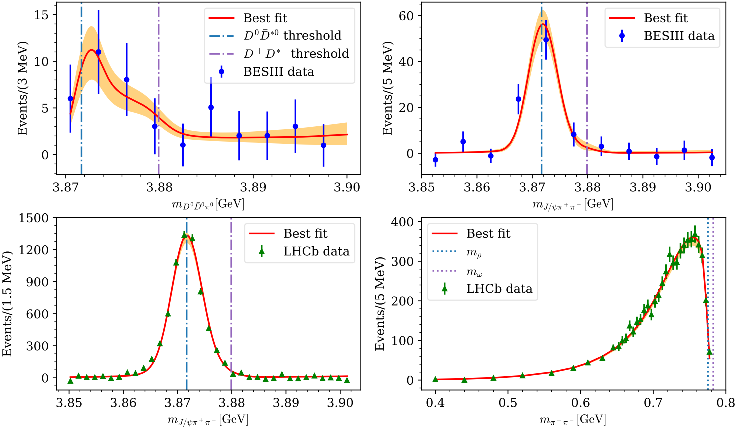

Experimental resolutions and efficiencies considered.
BESIII data on $e^+e^- \to \gamma(D^0\bar{D}^{*0}\pi^0/J/\psi\pi^+\pi^-)$ BESIII, arXiv:2309.01502,
LHCb data on $B \to K(J/\psi\pi^+\pi^-)$ LHCb, arXiv:2204.12597.
$\chi^2/\mathrm{dof} = 92.1/82 = 1.12$.

Pole positions of $X(3872)$ and W_{c1}^0

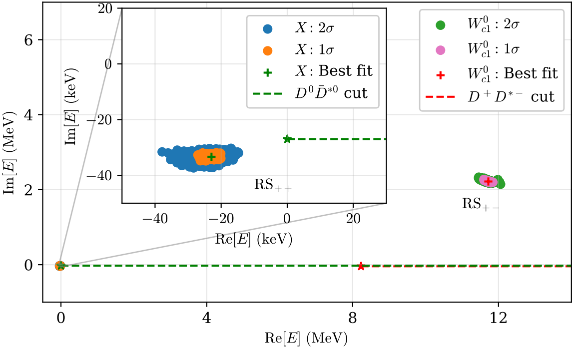

- Bound state of $D^0\bar{D}^{*0}$ with binding energy $E_X = (-22.9^{+2.8}_{-4.1} - i(33.3\pm1.5))$ keV.
- Another pole W_{c1}^0 on unphysical RS, virtual state, $E_W = (3.5\pm0.1 + i(2.2\pm0.1))$ MeV relative to D^+D^{*-} threshold.
- For comparison $E_X \sim \begin{cases} (25 - i\,140)\text{ keV (LHCb)} \\ (0 - i\,190)\text{ keV (BESIII)} \end{cases}$ with uncertainty $\mathcal{O}(100\text{ keV})$.

Decay widths of $X(3872)$

- From pole position,

$$\Gamma_{X\to D^0\bar{D}^{*0}} + \Gamma_{X\to J/\psi\, V} \approx 67 \text{ keV}.$$

- Tiny binding energy, $\Gamma_{X\to D^0\bar{D}^{*0}}$ constraint by D^{*0} width,

$$\Gamma_{X\to D^0\bar{D}^{*0}} = \Gamma_{X\to D^0\bar{D}^0\pi^0} + \Gamma_{X\to D^0\bar{D}^0\gamma} \sim \Gamma_{D^{*0}} \approx 55 \text{ keV}.$$

- The rest for $J/\psi\, V$,

$$\Gamma_{X\to J/\psi\, V} = \Gamma_{X\to J/\psi 2\pi} + \Gamma_{X\to J/\psi 3\pi} \approx 12 \text{ keV}$$

- $\text{Br}(X(3872)\to D^{*0}\bar{D}^0 + \text{ c.c. }) = \left(52.4^{+25.3}_{-14.3}\right)\%$ C. Li, et al. arXiv:1907.09149, we estimate

$$\Gamma_X = 80 \sim 120 \text{ keV}.$$

- More precious data are needed for other channels.

Isospin ~~breaking~~ of the $X(3872)$.

- Coupling of $X(3872)$ to each channel, $g_{X,\alpha} g_{X,\beta} = \lim_{E\to E_X}(E - E_X) T_{\alpha\beta}$,

$$g_{X,D^0\bar{D}^{*0}} = 0.20 + i0.02, \quad g_{X,D^+D^{*-}} = 0.16 + i0.02.$$

- By couplings,

$$\begin{aligned} X &\propto (g_{X,D^0\bar{D}^{*0}} + g_{X,D^+D^{*-}})\,|I=0\rangle + (g_{X,D^0\bar{D}^{*0}} - g_{X,D^+D^{*-}})\,|I=1\rangle \\ &\propto 9\,|I=0\rangle + |I=1\rangle \end{aligned}$$

- By calulating the ratio of $X \to J/\psi\rho$ and $X \to J/\psi\omega$ amplitudes,

$$R_X = 0.28 \pm 0.03.$$

- NOT match.
  Renormalization not well performed in $X \to D\bar{D}^*$ (loop) $\to$ J/ψV.
  To be fixed soon. R_X is the correct value.
- For $X(3872)$, mass eigenstate $\neq$ isospin eigenstate,
  non-negligible isospin-1 component.

Compositeness of $X(3872)$

- ERE at complex $D^0\bar{D}^{*0}$ threshold, $1/f = 1/a_0 - ik + r_0/2\,k^2 + \cdots$.

$$a_0 = (-28.4 \pm 2.0 + i\,(4.4 \pm 1.3))\ \text{fm},$$
$$r_0 = (0.9 \pm 0.1 + i\,(1.1 \pm 0.1))\ \text{fm}.$$

  For comparison,
  $a_0 \simeq -33$ fm, $-2.0 \lesssim r_0 \lesssim -5.3$ fm, LHCb, A. Esposito, et al. arXiv:2108.11413
  $a_0 = -16.5^{+7.0+5.6}_{-27.6-27.7}$ fm, $r_0 = -4.1^{+0.9+2.8}_{-3.3-4.4}$ fm, BESIII, arXiv:2309.01502

- Isospin breaking correction, V. Baru, et al. arXiv:2110.07484

$$\Delta r_{0,\mathrm{IB}} = \sqrt{\frac{\mu_2}{2\mu_1^2\Delta_{21}}} = 1.56\ \text{fm}.$$

- Compositeness I. Matuschek, et al. arXiv:2007.05329

$$\bar{X}_A = \left(1 + 2\left|\frac{\mathrm{Re}\, r_0 + \Delta r_{0,\mathrm{IB}}}{\mathrm{Re}\, a_0}\right|\right)^{-\frac{1}{2}} = 0.92 \pm 0.04$$

- Generalized formula Y. Li, et al. arXiv:2110.02766,
  $a_0 \in [-1/\sqrt{2\mu|E_B|}, 0]$ & $r_0 \leq 0$, Weinberg's formula holds
  $r_0 > 0$, $X = 1$ exactly, up to $\mathcal{O}(r_0/2\,k^2)$ in ERE.
- $X(3872)$ is a PURE molecule.

Contents

Summary

- Properties of the $X(3872)$ are studied preciously, in $J/\psi\pi^+\pi^-$ and $D^0\bar{D}^0\pi^0$ channels, LHCb 2022 and BESIII 2023.
- More reliable parameterization: unitarity and analyticity; coupled channels ($D\bar{D}^*$, $J/\psi V$); $D\bar{D}\pi$ 3-body effects (D^* dynamical widths, OPE).
  - Bound state of $D^0\bar{D}^{*0}$, $E_X = -23^{+3}_{-4}$ keV.
  - $\Gamma_X = 80 \sim 120$ keV. Partial decay widths. Data on other channels.
  - $R_X = 0.28 \pm 0.03$, much larger than $c\bar{c}$, ~ 0.05.
  - $\mathrm{Re}[r_0] > 0$, a PURE molecule.
  - Isospin partners $W_{c1}^{0,\pm}$, virtual states. Mild threshold cusps in $J/\psi\pi^\pm\pi^0$ channels.
  - $X(3872)$ and W_{c1}^0 contribute to the 1^{++} component at D^+D^{*-} threshold in $B^+ \to K^+D^\pm D^{*\mp}$ LHCb, arXiv:2406.03156? To be checked soon.

Thanks for your attention!

Backup Slides

TOPT of OPE

$$V^{\pi}(E;p',p) = \frac{g^2}{6F_\pi^2}\begin{pmatrix} \frac{1}{2}V^{SS}_{D^0\pi^0\bar{D}^0} & V^{SS}_{D^0\pi^+D^-} \\ V^{SS}_{D^+\pi^-\bar{D}^0} & \frac{1}{2}V^{SS}_{D^+\pi^0D^-}\end{pmatrix},$$

with

$$V^{SS}_{\alpha\beta\zeta} = \frac{1}{2}\int_{-1}^{1} dz \frac{q^2}{D^{\mathrm{TOPT}}_{\alpha\beta\zeta}(E;p',p,z)},$$

$$\frac{1}{D^{\mathrm{TOPT}}_{\alpha\beta\zeta}} = \frac{1}{2E_\beta(q)}\left(\frac{1}{D^R_{\alpha\beta\zeta}} + \frac{1}{D^A_{\alpha^*\beta\zeta^*}}\right),$$

$$D^R_{\alpha\beta\zeta} = \sqrt{s} - E_\alpha(p) - E_\beta(q) - E_\zeta(p') + i\varepsilon,$$

$$D^A_{\alpha^*\beta\zeta^*} = \sqrt{s} - E_{\alpha^*}(p') - E_\beta(q) - E_{\zeta^*}(p) + i\varepsilon.$$

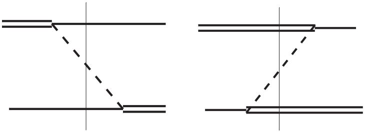

Energy-dependent widths of D^*

$$\Gamma_1(E;l) = \Gamma_{[D^{*0}\to D^0\gamma]} + \frac{g^2 M_{D^+}}{12\pi F_\pi^2 M_{D^{*0}}}\left[\Sigma_{D^+\pi^-D^0}(E;l,\mu_\pm) - \Sigma_{D^+\pi^-D^0}(0;0,\mu_\pm)\right] + \frac{g^2 M_{D^0}}{24\pi F_\pi^2 M_{D^{*0}}}\Sigma_{D^0\pi^0D^0}(E;l,\mu_0)\,,$$

$$\Gamma_2(E;l) = \Gamma_{[D^{*+}\to D^+\gamma]} + \frac{g^2 M_{D^+}}{24\pi F_\pi^2 M_{D^{*+}}}\Sigma_{D^+\pi^0D^-}(E;l,\mu_\pm) + \frac{g^2 M_{D^0}}{12\pi F_\pi^2 M_{D^{*+}}}\Sigma_{D^0\pi^+D^-}(E;l,\mu_\pm)\,.$$

with

$$\Gamma_{[D^{*0}\to D^0\gamma]} = 19.5\text{ keV},\quad \Gamma_{[D^{*+}\to D^+\gamma]} = 1.3\text{ keV},$$

$$\Sigma_{\alpha\beta\zeta}(E;l,\mu) = \left[2\mu_{\alpha\beta}\left(\sqrt{s} - M_\alpha - M_\beta - M_\zeta - \frac{l^2}{2\mu}\right)\right]^{3/2},$$

with $\mu_{\alpha\beta} = M_\alpha M_\beta/(M_\alpha + M_\beta)$.

Event distributions

$$\frac{\mathrm{d}\,\mathrm{Br}[D^0\bar{D}^0\pi^0]}{\mathrm{d}E} = \frac{1}{32\pi^3}\int_0^{p_{\max}} \frac{p\mathrm{d}p}{\omega_{D^0}(p)}\int_{\bar{p}_{\min}}^{\bar{p}_{\max}} \frac{\bar{p}\mathrm{d}\bar{p}}{\omega_{\bar{D}^0}(\bar{p})} \times \left(|T_{D^0\bar{D}^0\pi^0}(E,p,\bar{p})|^2 + f_{\mathrm{bg}}\right),$$

$$\frac{\mathrm{d}\,\mathrm{Br}[J/\psi\pi\pi]}{\mathrm{d}E} = \int_{2m_{\pi^+}}^{E-m_{J/\psi}} \frac{\mathrm{d}m_{2\pi}^2}{2\pi}\int \mathrm{d}\Phi_{2\pi}\frac{k_{J/\psi}(E,m_{2\pi})}{4\pi E}|T_{J/\psi\pi\pi}(E,m_{2\pi}^2,p_+)|^2,$$

$$\frac{\mathrm{d}\,\mathrm{Br}[J/\psi\pi\pi]}{\mathrm{d}m_{\pi\pi}} = \int \mathrm{d}E\int \mathrm{d}\Phi_{2\pi}\frac{k_{J/\psi}(E,m_{2\pi})m_{2\pi}}{4\pi^2 E}|T_{J/\psi\pi\pi}(E,m_{2\pi}^2,p_+)|^2,$$

Resolutions and efficiencies considered.

Fitted parameter values

Table: The parameter values and the correlation matrix from the best fit.

Parameters	Values	Covariance matrix								
P_1^{B}	2.6 ± 0.9	1.00								
$P_2^{\mathrm{B}}/P_1^{\mathrm{B}}$	0.7 ± 0.6	−0.86	1.00							
P_1^{L}	4.9 ± 1.0	0.68	−0.27	1.00						
$P_2^{\mathrm{L}}/P_1^{\mathrm{L}}$	0.54 ± 0.06	−0.09	0.04	−0.24	1.00					
C_{0X}	-3.06 ± 0.05	0.37	−0.17	0.49	−0.08	1.00				
C_{1X}	-9.47 ± 0.60	−0.01	0.03	0.04	−0.01	−0.84	1.00			
f_{bg}	4 ± 6	−0.18	−0.03	−0.35	0.04	−0.19	0.01	1.00		
a	1.3 ± 0.4	0.05	−0.04	0.04	−0.05	0.66	−0.78	−0.03	1.00	
u	-0.83 ± 0.26	0.49	−0.20	0.69	−0.08	0.87	−0.62	−0.26	0.71	1.00